

# A study of nuclear stopping in central symmetric nuclear collisions at intermediate energies

C. Escano-Rodriguez,<sup>1</sup> D. Durand,<sup>2</sup> A. Chbihi,<sup>1</sup> J.D. Frankland,<sup>1</sup> M.L. Begemann-Blaich,<sup>3</sup> R. Bittiger,<sup>3</sup> B. Borderie,<sup>4</sup> R. Bougault,<sup>2</sup> J.-L. Charvet,<sup>5</sup> D. Cussol,<sup>2</sup> R. Dayras,<sup>5</sup> E. Galichet,<sup>4,6</sup> D. Guinet,<sup>7</sup> P. Lautyresse,<sup>7</sup> A. Le Fèvre,<sup>3</sup> R. Legrain,<sup>5,\*</sup> N. Le Neindre,<sup>4</sup> O. Lopez,<sup>2</sup> J. Łukasik,<sup>3</sup> U. Lynen,<sup>3</sup> L. Manduci,<sup>2</sup> W.F.J. Müller,<sup>3</sup> L. Nalpas,<sup>5</sup> H. Orth,<sup>3</sup> M. Pärlog,<sup>8</sup> M. F. Rivet,<sup>4</sup> E. Rosato,<sup>9</sup> R. Roy,<sup>10</sup> A. Saija,<sup>3</sup> C. Schwarz,<sup>3</sup> C. Sfienti,<sup>3</sup> B. Tamain,<sup>2</sup> W. Trautmann,<sup>3</sup> A. Trzcinski,<sup>11</sup> K. Turzó,<sup>3</sup> E. Vient,<sup>2</sup> M. Vigilante,<sup>9</sup> C. Volant,<sup>5</sup> J.P. Wieleczko,<sup>1</sup> and B. Zwieglinski<sup>11</sup>

(INDRA and ALADIN collaborations)

<sup>1</sup> GANIL, CEA et IN2P3-CNRS, B.P. 55027, F-14076 Caen Cedex, France.

<sup>2</sup> LPC, IN2P3-CNRS, ENSICAEN et Université, F-14050 Caen Cedex, France.

<sup>3</sup> Gesellschaft für Schwerionenforschung mbH, D-64291 Darmstadt, Germany.

<sup>4</sup> Institut de Physique Nucléaire, IN2P3-CNRS, F-91406 Orsay Cedex, France.

<sup>5</sup> DAPNIA/SPhN, CEA/Saclay, F-91191 Gif sur Yvette Cedex, France.

<sup>6</sup> Conservatoire National des Arts et Métiers, F-75141 Paris Cedex 03.

<sup>7</sup> Institut de Physique Nucléaire, IN2P3-CNRS et Université F-69622 Villeurbanne, France.

<sup>8</sup> National Institute for Physics and Nuclear Engineering, RO-76900 Bucharest-Măgurele, Romania.

<sup>9</sup> Dipartimento di Scienze Fisiche e Sezione INFN,

Università di Napoli "Federico II", I-80126 Napoli, Italy.

<sup>10</sup> Laboratoire de Physique Nucléaire, Université Laval, Québec, Canada.

<sup>11</sup> Soltan Institute for Nuclear Studies, PL-00681 Warsaw, Poland.

(Dated: Revision : 1.2 Date : 2005/01/2109 : 24 : 34)

Nuclear stopping has been investigated in central symmetric nuclear collisions at intermediate energies. Firstly, it is found that the isotropy ratio,  $R_{iso}$ , reaches a minimum near the Fermi energy and saturates or slowly increases depending on the mass of the system as the beam energy increases. An approximate scaling based on the size of the system is found above the Fermi energy suggesting the increasing role of in-medium nucleon-nucleon collisions. Secondly, the charge density distributions in velocity space,  $dZ/dv_{||}$  and  $dZ/dv_{\perp}$ , reveal a strong memory of the entrance channel and, as such, a sizeable nuclear transparency in the intermediate energy range. Lastly, it is shown that the width of the transverse velocity distribution is proportional to the beam velocity.

The study of transport phenomena in nuclear reactions at intermediate energies is of major importance in the understanding of the fundamental properties of nuclear matter (for an introduction see[1]). The comparison of the predictions of the microscopic transport models (see for instance [2, 3, 4, 5, 6]) with experimental data can help improve our knowledge of the basic ingredients of such models: namely the nuclear equation of state and as such, the in-medium properties of the nucleon-nucleon interaction. In this context, it is mandatory to test the different models over a large systematics in system size and incident energy. Among the different issues that can be addressed in such a framework, the question of the thermalization of the system (in particular the damping of the momentum distribution) in strongly dissipative collisions is among the most debated in view of its connection with the search for a phase transition of the liquid-gas like type[7, 8].

In this paper, we investigate this problem by studying the stopping power in nuclear reactions at intermediate energies. We take advantage of the high quality of the data collected for a large variety of systems with the INDRA multidetector both at GANIL (see for instance [9, 10, 11, 12, 13]) and at GSI [14, 15]. Symmetric sys-

tems with total sizes between 80 and 400 mass units and with incident energies between 25 and 100A MeV have been considered. Event selection is performed as follows: in view of the experimental detection thresholds in the backward part of the detection device, we have only considered charged products which are emitted in the forward velocity space in the centre-of-mass of the reaction. In this way the effect of the thresholds are minimized as well as the associated distortions on the global variables considered in the following. The selection criterium as far as the quality of the data is concerned was the following: events were retained if the total detected charge,  $Z_{tot}$  (neutrons were not detected) in the forward hemisphere of the centre-of-mass was larger than 90% of half the total charge of the considered system. Contrarily to the study of the FOPI data presented in [16], no attempt has been made to symmetrize the data.

In the following, we concentrate on central collisions. This raises the question of the selection of those events on criteria which do not induce auto-correlations. Since we are interested in quantities involving both the transverse and longitudinal directions, it is not suitable to use vector variables such as, for instance, the transverse energy [10, 17]. Thus, a scalar variable is needed and the

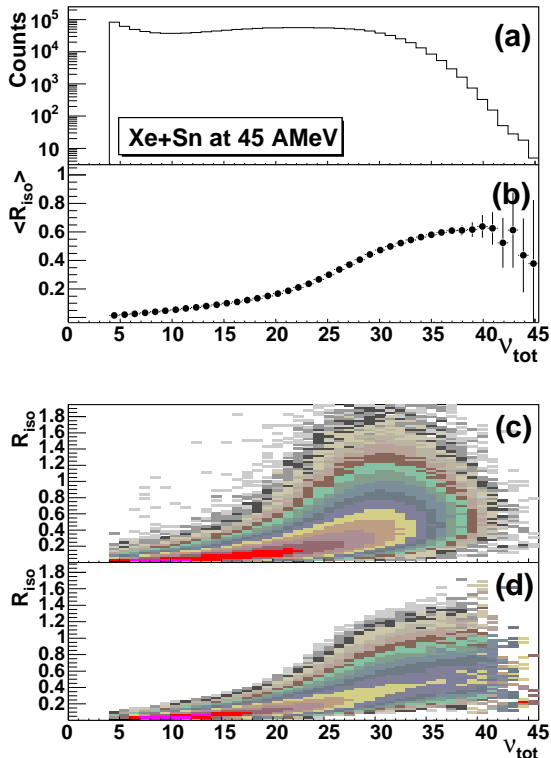


Figure 1: Data for Xe+Sn collisions at 45A MeV: (a) Distribution of total charged particle multiplicity  $\nu_{tot}$ . (b) Evolution of the mean isotropy ratio  $R_{iso}$  as a function of the total multiplicity,  $\nu_{tot}$ . (c) Bi-dimensional plot showing the correlation between the isotropy ratio and the total multiplicity. Different intensities (in log scale) represent different numbers of measured events. (d) As (c), but after renormalising the number of events in each bin according to the evolution of the cross-section with the multiplicity from (a).

most natural one is the multiplicity of detected charged products,  $\nu_{tot}$ . In that sense, a minimum bias selection is used. We now consider the isotropy ratio,  $R_{iso}$ , defined as :

$$R_{iso} = \frac{\sum E_{\perp}}{2 \sum E_{\parallel}} \quad (1)$$

where  $E_{\perp}$  ( $E_{\parallel}$ ) is the c.m. transverse (parallel) energy and the sum runs over all products with the above-mentioned selection. We first consider the evolution of  $R_{iso}$  as a function of  $\nu_{tot}$ . Another possibility was to consider the evolution as a function of the particle multiplicity emitted in the forward direction but this does not affect the conclusions. The four panels in Figure 1 illustrate the selection method of the central collisions. Figure 1a shows the distribution of  $\nu_{tot}$  while Figure 1b displays the evolution of the mean value of  $R_{iso}$  as a function of  $\nu_{tot}$ . The mean value of  $R_{iso}$  displays a S-like shape and reaches an asymptotic value hereafter noted

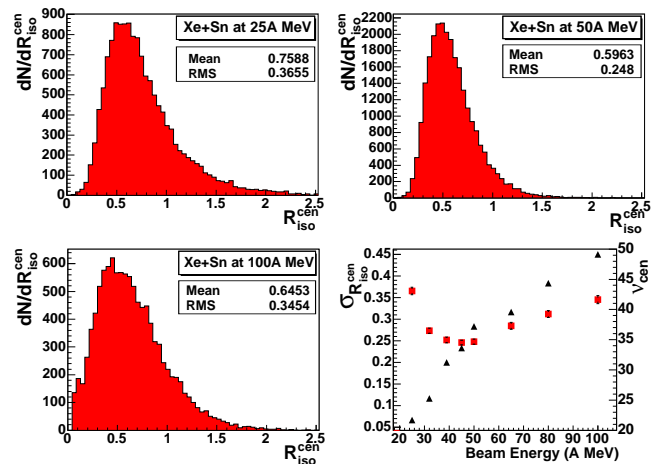


Figure 2: Distribution of  $R_{iso}^{cen}$  in Xe+Sn central collisions. The incident energy, mean value and variance of  $R_{iso}^{cen}$  are indicated in each panel. The last panel shows the evolution of the RMS (squares and left scale) while triangles and the right scale correspond to  $\nu_{cen}$  defined in the text. Note that both scales do not start from zero.

$R_{iso}^{cen}$ , and its corresponding mean value  $\langle R_{iso}^{cen} \rangle$ , for the largest values of  $\nu_{tot}$ . Strong fluctuations are observed for extreme values of  $\nu_{tot}$  where the statistics is very low (typically less than 10 events, see Figure 1a). In the following, we calculate the asymptotic value of  $R_{iso}$  by considering the mean value of  $R_{iso}$  for events with a multiplicity larger than  $\nu_{cen}$  (these are plotted as a function of the incident energy as triangles (right scale) in the last panel of Figure 2).  $\nu_{cen}$  is defined as the multiplicity of charged products at which  $R_{iso}$  reaches its asymptotic value. Figures 1c and 1d show the bi-dimensional correlation between  $\nu_{tot}$  and  $R_{iso}$ . It is worth noting from Fig. 1c that the largest fluctuations of  $R_{iso}$  are not associated with the largest values of the multiplicity. This could suggest that the selection of central events by means of  $\nu_{tot}$  is inappropriate. Let us discuss briefly this point. A first effect to consider is the influence of the statistics of the multiplicity distribution : this has been accounted for in Fig. 1d by dividing the contents of each bin by the number of events with the corresponding multiplicity obtained from Fig. 1a. The large fluctuations observed for intermediate values of the multiplicity have disappeared demonstrating that this effect is to a large extent due to statistics.

Another argument in favour of the present selection of central collisions concerns the velocity-dependent charge densities [18, 19] (defined later in this paper). Such distributions (not shown here except for central collisions, see Figure 4) do not change anymore for multiplicities  $\nu_{tot} \geq \nu_{cen}$ . This shows that for multiplicities larger than  $\nu_{cen}$ , the events have the same kinematical characteristics and that they only differ by the sorting variable, namely the multiplicity. We call these events "central

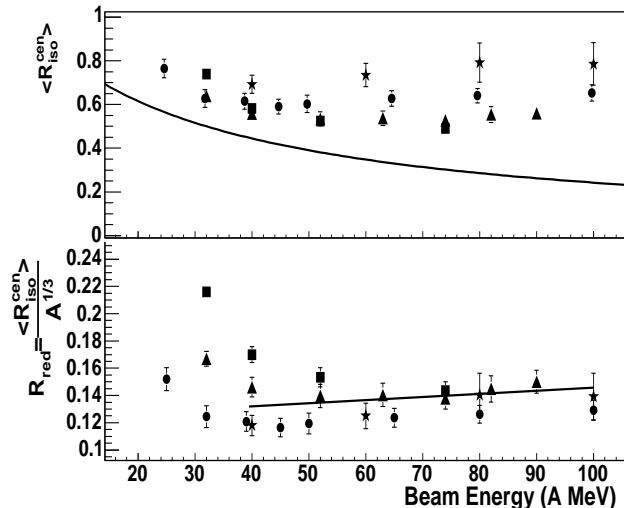


Figure 3: Top: Evolution of the mean value of  $R_{iso}^{cen}$  (and the associated uncertainty) as a function of the beam energy for central collisions and for various systems: (stars) Au+Au, (dots) Xe+Sn, (triangles) Ni+Ni and (squares) Ar+KCl. The solid line is the value of  $R_{iso}$  corresponding to the initial nucleon momentum distributions consisting of two sharp Fermi spheres separated by a relative velocity corresponding to the considered beam energy. Bottom: Same as above for the scaled isotropy ratio:  $\langle R_{iso}^{cen} \rangle / A^{1/3}$ . The solid line is a linear fit to all data points above 40 A MeV.

events": they correspond to roughly 1% of the reaction cross-section and are the only events considered in the following.

The present study has been undertaken for a variety of systems in the intermediate energy range. Let us first consider the nearly symmetric Xe+Sn system. Figure 2 shows examples of  $R_{iso}^{cen}$  distributions between 25 and 100 A MeV incident energy. The distributions are not gaussian-like and the most probable values do not drastically change and remain close to 0.5-0.6 as the beam energy increases. The evolution of the mean value is thus to a large extent governed by the evolution of the width of the distributions. These latter are plotted in the last panel (squares and left scale). A minimum is observed near 40-50 A MeV close to the Fermi energy. Also shown are the values of  $\nu_{cen}$  (triangles) in the last panel. They increase from about 22 at 25 A MeV up to 47 at 100 A MeV.

Figure 3 shows the evolution of  $\langle R_{iso}^{cen} \rangle$  for various symmetric systems whose total sizes vary from about 80 up to 400 mass units. The upper panel of the figure shows that, below 40 A MeV, the isotropy ratio is nearly independent of the size of the system and slowly decreases. However, as the beam energy crosses the Fermi energy, one observes an increase of the isotropy ratio depending on the size of the system: the larger the size, the larger  $\langle R_{iso}^{cen} \rangle$ . The solid line on Figure 3-top is the value

of the isotropy ratio in the entrance channel due to the Fermi distribution of the nucleons inside the projectile and the target. Thus, the distance between the experimental points and the solid line is a "measure" of the influence of the dissipation on the isotropy ratio.

The general evolution of the data is interpreted as a transition from the dominant influence of the mean field at low energy (one-body dissipation which does not depend on the size of the system) towards the dominance of in medium nucleon-nucleon collisions at higher energy (two-body dissipation which depends on the size of the system).

In this case, the key quantity is the ratio between the nucleon mean free path and the size of the system. This is tentatively put in evidence in Figure 3 (lower panel) where the reduced isotropy ratio  $R_{red} = \langle R_{iso}^{cen} \rangle / A^{1/3}$  has been plotted for all considered systems (here  $A$  has been arbitrarily taken as half the total mass of the system as we are dealing with symmetric systems). For medium and heavy systems (Xe+Sn and Au+Au), the scaling is evidenced for beam energies larger than 40-50 A MeV while for lighter systems (Ar+KCl and Ni+Ni), it is more and more verified as the beam energy increases. These features outline the role of the size of the system as far as the damping of the nucleon momentum distribution is concerned. This scaling and the rather low values of  $\langle R_{iso}^{cen} \rangle$  suggest that the mean free path of the nucleons inside the medium is rather long at such incident energies. It is of the same order of magnitude or even larger than the size of the system. One should also have in mind surface effects in the sense that even for central collisions, those nucleons that are more localized in the vicinity of the surface have little chance to experience hard collisions: All in all, this means that two-body dissipation is not enough to drive the system towards thermalization.

Up to now, we have only considered a global variable,  $R_{iso}$ , built on an event by event basis. We now consider a variable which is averaged over all the selected events: namely the velocity-dependent charge density,  $dZ/d\eta_{\parallel}^{red}$  and  $dZ/d\eta_{\perp}^{red}$  respectively along the beam axis and along one of the transverse directions. These quantities are built by considering all charged particles emitted in the forward centre of mass direction, adding the particles (weighted with their respective nuclear charges) which are localized in the same velocity bin. These distributions are well-suited to a comparison with microscopic transport models, as shown for instance in [19]. The same distributions have been studied for FOPI data in [16]. In order to compare easily the same system at different beam energies, scaled velocities have been used:  $\eta = v/v_{cm}$  where  $v_{cm}$  is the projectile velocity in the centre-of-mass frame.

Figure 4 shows the evolution of the two densities for the system Xe+Sn at various incident energies between 25

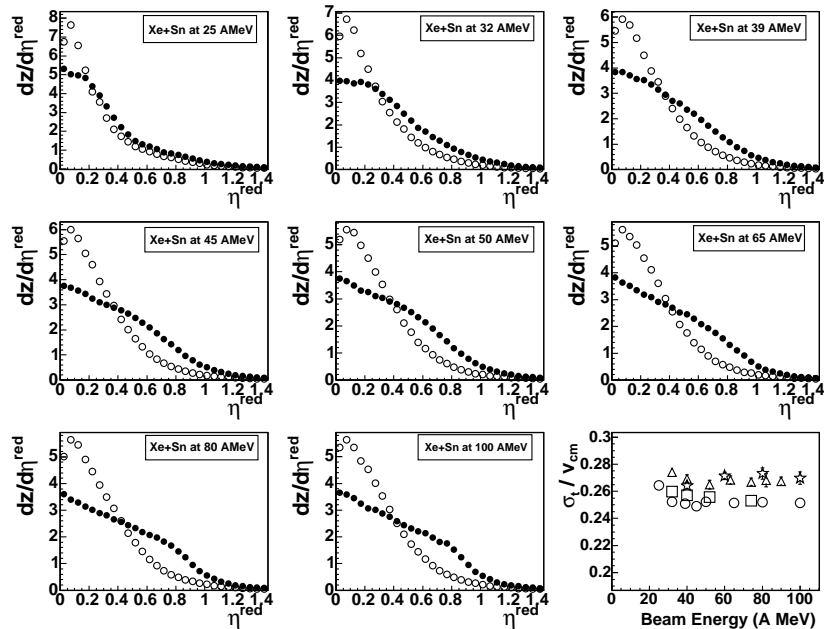


Figure 4: Top:  $dZ/d\eta_{\parallel}^{red}$  (black points) and  $dZ/d\eta_{\perp}^{red}$  (open points) in the parallel and in one of the two transverse directions for central Xe+Sn collisions for various incident energies indicated in each panel. The distributions are normalized in such way that the total charge corresponds approximately to half the total charge of the system. Last panel: Evolution as a function of the incident energy of the width of the charge density distribution in the transverse direction, for (stars) Au + Au, (circles) Xe + Sn, (triangles) Ni + Ni and (squares) Ar + KCl systems.

and 100A MeV. There is a clear correlation between  $R_{iso}$  and the behaviour of the two charge densities. Even at 25A MeV, the two distributions are not identical, which would indicate the occurrence of full stopping. However, this is the incident energy for which the two distributions are the closer to each other and consequently, it corresponds to the largest value of  $R_{iso}$ . For all the considered energies, a strong memory of the entrance channel is evidenced: the widths of  $dZ/d\eta_{\parallel}^{red}$  are larger than the widths of  $dZ/d\eta_{\perp}^{red}$ . A closer look at the transverse distributions shows that they are quite similar whatever the incident energy. This is illustrated in the last panel of Figure 4. The reduced width of  $dZ/d\eta_{\perp}^{red}$  shows a remarkable constancy as a function of the incident energy indicating that the transverse collective motion is proportional to the beam velocity. Moreover there is no significant dependence on the size of the system, the same constancy is observed for other systems with different sizes : Au + Au, Ni + Ni and Ar + KCl (see Figure 4, last panel). It would be interesting to study the origin of this effect in microscopic transport calculations.

To conclude, we have studied the behaviour of two observables, the isotropy ratio  $R_{iso}$  and the velocity-dependent charge density  $dZ/d\eta^{red}$ ; in central symmetric nuclear reactions at intermediate energies. The evolution of  $R_{iso}$  as a function of the incident energy shows a minimum followed by a moderate increase for most studied systems or a plateau around the Fermi energy for the lightest ones. Rather low values have been measured indi-

cating that full stopping is far from being achieved in this energy regime. As far as medium-mass and heavy systems are considered, a scaling law in terms of the size of the system is observed suggesting the role of in-medium nucleon-nucleon collisions in the slow increase of the stopping power. The study of the velocity-dependent charge density in the parallel and transverse directions with respect to the beam shows a strong memory of the entrance channel in the sense that the densities in the parallel and transverse directions do not coincide suggesting transparency as a key feature of nuclear reactions at intermediate energies. Last, the width of the transverse charge density using reduced velocities is invariant in the entire intermediate energy range.

Our findings concerning the stopping power in central nuclear collisions are in full agreement with a recent study based on very similar observables performed by the FOPI Collaboration at higher incident energies up to the GeV region [16]. Our results as well as those of FOPI should be compared with the predictions of existing microscopic transport models. As such, we believe that they constitute a very severe test of these models over a wide range of system sizes and incident energies.

---

\* deceased

[1] D. Durand, B. Tamain, and E. Suraud, *Nuclear Dynam-*

- ics in the Nucleonic Regime* (Institute Of Physics, 2001).
- [2] A. Ohnishi and J. Randrup, Phys. Rev. Lett. **75**, 596 (1995).
  - [3] J. Aichelin, Phys. Rep. **202**, 233 (1991).
  - [4] A. Bonasera *et al.*, Phys. Rep. **243**, 1 (1994).
  - [5] P. Chomaz, *et al.*, Phys. Rev. Lett. **73**, 3512 (1994).
  - [6] A. Ono, *et al.*, Phys. Rev. Lett. **68**, 2898 (1992).
  - [7] B. Borderie, J. Phys. G: Nucl. Part. Phys. **28**, R217 (2002).
  - [8] M. D'Agostino *et al.*, Nucl. Phys. **A724**, 455 (2003).
  - [9] N. Marie, *et al.* (INDRA collaboration), Phys. Lett. **B 391**, 15 (1997).
  - [10] E. Plagnol, *et al.* (INDRA collaboration), Phys. Rev. **C 61**, 014606 (1999).
  - [11] V. Métévier, *et al.* (INDRA collaboration), Nucl. Phys. **A 672**, 357 (2000).
  - [12] B. Borderie, J. Phys. G: Nucl. Part. Phys. **28**, R217 (2002).
  - [13] S. Hudan, A. Chbihi, J. D. Frankland, *et al.* (INDRA collaboration), Phys. Rev. **C 67**, 064613 (2003).
  - [14] J. Łukasik, *et al.* (INDRA and ALADIN collaborations), Phys. Rev. **C 66**, 064606 (2002).
  - [15] A. Le Fèvre, *et al.* (INDRA and ALADIN collaborations), Nucl. Phys. **A 735**, 219 (2004).
  - [16] W. Reisdorf *et al.* (FOPI), Phys. Rev. Lett. **92**, 232301 (2004).
  - [17] J. Łukasik, *et al.* (INDRA collaboration), Phys. Rev. **C 55**, 1906 (1997).
  - [18] J. F. Lecomte, *et al.* (INDRA collaboration), Nucl. Instr. and Meth. in Phys. Res. **A 441**, 517 (2000).
  - [19] E. Galichet, *et al.* (INDRA collaboration), Eur. Phys. J. **A 18**, 75 (2003).